A DYNAMIC COUPLED THERMAL AND ELECTRICAL MODEL OF RESIDENTIAL ROOFTOP BIPV SYSTEMS

Ya Brigitte Assoa[1], Thierry Guiot[2], Leon Gaillard[3, 4], Benjamin Boillot[1], Christophe Ménézo[3]
[1]LEB/DTS/CEA-INES RDI : Bâtiment LYNX 1, 73377 Le Bourget du Lac, France
[2]Centre Scientifique et Technique du Bâtiment (CSTB), 06904 Sophia Antipolis, France
[3]Centre de Thermique de Lyon CETHIL UMR 5008, Chaire INSA de Lyon/EDF « Habitat et innovations Energétiques », 69621 Villeurbanne, France
[4]LOCIE CNRS UMR 5271, Polytech'Savoie, Le Bourget du Lac, France

ABSTRACT

We present a transient coupled thermal and electrical model of BIPV systems installed on rooftops and naturally ventilated through air cavities imposed by building conception rule (ventilation of skeleton). This model realized in TRNSYS software was experimentally validated using five different residential BIPV systems commercially available in France in 2010. Relative differences between predicted and measured data exceeding 2% and 4% were observed for the thermal and electrical results respectively. The model was accurate to 2% for sunny days and less precise for cloudy days. This model was used to deduce the impact of rooftop integration configuration on electrical performance.

INTRODUCTION

As part of the "20-20-20" energy and climate change objectives adopted in 2007, the European Union aims to increase the share of renewable energy to 20% by 2020 (EC, 2010). Photovoltaic (PV) systems are expected to contribute increasingly to this transformation, as their economic viability improves relative to other energy technologies (Schleicher-Tappeser, 2012). Accounting for a major portion of energy consumption in the Union, the construction sector has been target with specific regulatory frameworks to improve the energy efficiency of buildings in part by the integration of renewable energy technologies. For example on a national level, the British Code for Sustainable Homes (DCLG, 2010) and the French Thermal Regulation (MEDDE, 2012) both provide incentives for renewable energy.

In Europe, national and regional energy policy is driving greater uptake of photovoltaic systems into urban landscapes. This move towards a decentralisation of energy supplies is however, limited by certain technical and economic constraints. In particular, there is an urgent need for reliable predictions of energy generation from building-integrated photovoltaic (BIPV) systems, which owe a more complex behaviour to the thermal interaction with the building.

In France, residential BIPV systems have been particularly promoted, and this is reflected by the current inventory of PV installation in the country (Leloux et al., 2012).

Different forms of integration are offered by the various BIPV systems available in France, ranging from classic arrangements of PV modules attached on top of an existing rooftop, to fully-integrated systems, where photovoltaic modules essentially replace building components and thereby provide cover and weather protection in addition to generating electricity. Despite the opportunities presented by fully-integrated systems, this configuration may result in a higher module operating temperature than for openly ventilated PV modules (Fuentes, 1987). This limitation has motivated research efforts to optimise the cooling of PV modules by extracting dissipated heat, and typical BIPV systems include most of the time, an insulated air layer which promotes PV modules cooling by natural ventilation. The objective of this ventilation is to maintain the performance of building-integrated PV modules at a level equivalent to that of non-integrated systems given that in traditional rooftop, natural ventilation is mandatory to avoid moisture onto thermal insulation.

In recent years, experimental and theoretical studies have been directed to the investigation of various building integrated PV configurations and applications (Bazilian et al., 2001). In 2003, Chow (Chow, 2003) developed a transient physical model for a hybrid PV/T collector comprising a circulating water heat exchanger welded to a metal absorber incorporated into the rear of a PV module. In 2006, Tiwari et al. presented theoretical and experimental studies of a solar PV/T air collector. This component consists of photovoltaic modules connected in series and mounted on a non-corrosive Tedlar layer. An air gap insulated with wood permits the natural or forced ventilation of the PV modules on the underside (Tiwari et al., 2006).

In 2003, Barker and Norton (Barker and Norton, 2003) used the thermal model proposed by Ingersoll (Ingersol, 1986) to estimate the PV module thermal behaviours for four mounting configurations.

In this paper, we present a dynamic thermal and electrical model for BIPV systems typical of detached residential properties in France. The

components studied in this work are opaque polycrystalline solar photovoltaic modules integrated into a tilted and insulated tiled rooftop, with PV modules and the insulation layer separated by a naturally ventilated air gap. The simulation tool was developed as part of the ANR HABISOL "Performance BIPV" research program. The research project also included the installation and monitoring of seven full-scale BIPV test benches for a period of one year. The data from these test benches were used to validate the models, and to identify the global thermal characteristics of different integration classes.

SIMULATION

A coupled thermal-electrical nodal model

The dynamic modelling of residential rooftop BIPV system was pursued by first developing separate models for the thermal and electrical behaviours of the system. The models were then coupled within TRNSYS 17 software environment, by using PV module temperatures calculated by the thermal model as inputs to the electrical model, and the absorbed heat calculated by the electrical model as an input to the thermal model. A schematic representation of the coupled model is presented in Figure 1. The thermal and electrical models were coupled using the standard TRNSYS solver algorithm, corresponding to the method of successive substitution.

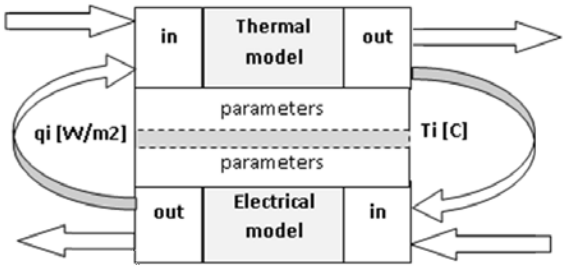

Figure 1 Input-output diagram of the coupled thermal-electrical model for a BIPV system

Simulation of thermal behaviour

For the thermal model, a 2D nodal approach was applied, which reduced the BIPV system to the arrangement shown in Figure 2. The model makes the following assumptions: the insulation layer at the underside of the air gap is initially assumed adiabatic; only a portion of collector along the roof is modelled taking into account the upper and lower tiles; the air gap is discretized along the roof in equal finite volumes and PV modules are represented by a single temperature node per finite volume. Additionally, in order to improve the convergence stability of the heat balance algorithm, the heat capacity of the air temperature node in the gap is assumed to be negligible. The direction of air flow in the gap was considered by adding a sign to the air mass flow into the heat balance equation.

For each finite volume, a heat balance is obtained for the temperature nodes of the PV modules (Tmo, i), of the air in the gap (Tfl, i) and for the insulation layer surface (Tfd, i) (see Figure 1). The heat balance at the central temperature node of each PV module, for a finite volume i, is given by Equation 1.

$$M_{mo,i}\frac{dT_{mo,i}}{dt} = q\cdot L + K_{a,mo,i}\left(T_a - T_{mo,i}\right) + K_{s,mo,i}\left(T_s - T_{mo,i}\right) + K_{gnd,mo,i}\left(T_{gnd} - T_{mo,i}\right) + K_{fd,i,mo,i}\left(T_{fd,i} - T_{mo,i}\right) + K_{fl,mo,i}\left(T_{fl,i} - T_{mo,i}\right) \quad (1)$$

The heat balance at the air temperature node in the gap is given by:

$$T_{fl,i} = \frac{\dot{m}\cdot C_p\cdot T_{fl,i-1} + K_{fl,ar}\cdot T_{ar,i} + K_{fl,fd}\cdot T_{fd,i}}{\dot{m}\cdot C_p + K_{fl,ar} + K_{fl,fd}} \quad (2)$$

The inlet air Tfl,0 is assumed to be at the same temperature as ambient air Ta.

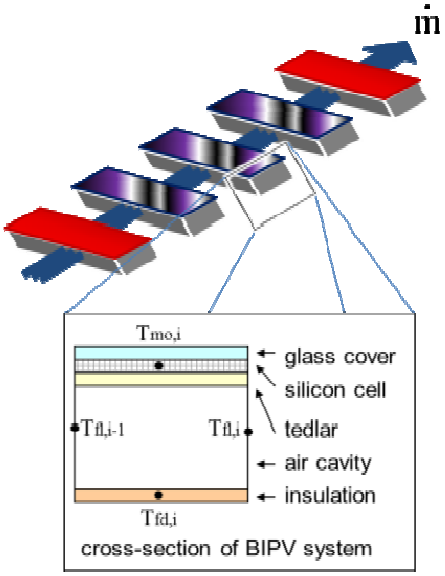

Figure 2 The discretization of BIPV systems applied for the thermal model. The elemental transversal section of the system is shown in the enlarged frame.

The thermal balance of the nodal model is sought iteratively with a simplified aerodynamic model to describe air flow in the cavity. Following the approaches of Brinkworth and Sandberg (Brinkworth et al., 2000) and (Sandberg et al., 1998), the model is constructed by evaluating the buoyancy-induced pressure difference of each discretized zone, and equating this to pressure losses arising from the inlets and friction inside the cavity. Defining the buoyancy thrust in terms of the mean air temperature of each zone relative to ambient air, and allowing friction to vary with mass flow rate, aerodynamic balance is thus defined.

$$\frac{1}{2}\frac{\dot{m}^2}{\rho.H^2}\left(X+\sum L_i\frac{f_i(Re_i)}{2.H}\right).sign(\dot{m}) = \rho.\beta.(0.5.(T_{fl,i}+T_{fl,i-1})-T_a).g.L_i.\sin(\beta) + \frac{1}{2}\Delta C_p.\rho.V^2 \quad (3)$$

Where Tfl,i is here the mean air temperature in zone i (approximated as the simple mean of temperatures at the zone boundary. The last term describes the wind effect, defined in terms of the net wind coefficient on inlets and the local mean wind speed.

In order to appropriately configure the thermal model, computation fluid dynamics calculations (CFD) were used to estimate pressure loss coefficients and heat transfer coefficients.

Electrical modelling

The electric model was based on commonly used 1-diode current-voltage models available in TRNSYS. This choice was motivated in order to test the validity of such models when applied to the scenario of BIPV systems. Rather than imposing a common average array temperature, the model was extended to allow individual module temperatures to be used, so that the possible impact to array thermal and electrical performance could be considered. The model therefore included an algorithm to solve a series combination of PV modules with varying radiation and temperature conditions. The PV array is assumed to be grid connected via a dedicated inverter.

The voltage-current model consists of a simplified one diode electrical circuit (comprising resistors connected in series and in parallel), described by Equation 3. The model is thus defined by five parameters: I_L, I_0, γ, R_s, and R_{sh}.

$$I = I_L - I_0\left(\exp\left[\frac{q(V+R_sI)}{\gamma k T_c}\right]-1\right)-\frac{V+R_sI}{R_{sh}} \quad (4)$$

The five intrinsic parameters of these equations are estimated using the module characteristics provided by manufacturers. In the present study, two different algorithms were considered, both available in TRNSYS: the model based on Duffy et al. work (Duffy et al., 1991), and the more elaborate model based on De Soto et al. model (De Soto et al., 2006). The two methods were compared using flash test data of the 84 modules constituting the seven BIPV test benches. The simpler electrical model was selected for further study due to the following two key findings. Firstly, the physical variation between modules of the same make was comparable to the systematic variation between models. Secondly, model-derived linear temperature coefficients at standard radiation were found to be insensitive to the variation in coefficients reported by the manufacturers.

For a given incident radiation and module temperature, the five model parameters were modified, using correlations in terms of their values at reference conditions (S_{ref}=1000 W/m^2 and T_a=25 °C). The following Equations 5 to 10 are used to change these parameters settings depending on the radiation and PV module temperature for the selected model.

$$I_L = (S_{eff}/S_{ref})\cdot(I_{L,ref}+\alpha_{Isc}(T_c-T_{c,ref})) \quad (5)$$

$$I_L = I_{0,ref}(T_c/T_{c,ref})^3 \cdot\exp\left[(1/k_b)\left((E_{g,ref}/T_{c,ref})-(E_g/T_c)\right)\right] \quad (6)$$

$$E_g = E_{g,ref}(1-0.0002677(T_c-T_{c,ref})) \quad (7)$$

$$\gamma = \gamma_{ref}(T_c/T_{c,ref}) \quad (8)$$

$$R_{sh} = R_{sh,ref}(S_{ref}/S_{eff}) \quad (9)$$

$$R_s = R_{s,ref} \quad (10)$$

The temperature dependence of the parameters γ and R_{sh} were ignored for the simpler model.

For homogeneous environmental conditions and identical modules, the power generation of a PV array is equal to the sum of that of each module. In order to take into account any temperature differences between modules in a BIPV field, a one dimensional electrical model was developed. This model permits for a field of N identical PV modules in series, the evaluation of each module the voltages and the common current for a given global voltage. The field is defined by the N-1 electrical interconnection and by the sum of the individual voltages. This vector is solved by one dimension Newton-Raphson iteration. In order to accelerate the calculation, Equation 3 was transformed into an explicit solution, following the approach presented by Piccault et al. (Piccault et al., 2010).

For the series arrays of crystalline silicon modules considered in the current project, and the temperature gradients that were observed to develop (nearly 10°C maximum temperature difference between upper and lower rows of modules), thermal mismatch effects were found to have a negligible impact on produced power, relative to a zero-dimensional model using mean array temperature. This is explained by the fact that thermal sensitivity for module current is very limited compared to voltage sensitivity the later being well described by a linear behaviour so that averaged temperature is a sufficient representation. The 1D solution was thus retained as an optional mode in the calculation, in order to test sensitivity of the thermal model to local heat flux.

EXPERIMENT

Model validation was undertaken using data from seven BIPV test benches that were monitored for a period of one year, with minute-wise measurements of thermal and electrical characteristics recorded from 03:00 to 20:00 each day. Six systems were constructed at the INES site at Le Bourget du Lac (see Figure 3), and one at CSTB, Sophia Antipolis. The test benches comprised a metal support structure consisting of a 35 m² tray mounted on a 3.70 m high base, and inclined on one axis in the interval [0°, 50°] to horizontal. Prior to installation of the BIPV systems, all modules were analysed by flash-test at standard radiation. Inverters and sensors were similarly characterised prior to use. Calibration of temperatures and electrical measurements were made channel by channel.

Figure 3 Test benches on INES site at Le Bourget du Lac

Each BIPV system was instrumented in the same fashion. Electrical output to either side of the inverters was measured using by Hall-effect sensors (DC) and shunts. Thermocouples were attached to the back sheet of each module, close to the centre of the module and strictly behind a cell. An epoxy resin impregnated with aluminium powder was used to attach the thermocouples, a medium offering a similar emissivity to the back sheet. Module back sheets were cleaned prior to fixing the thermocouples. Ambient temperature was measured using a Pt100 sensor sheltered from solar radiation, in accordance with the protocols of the French Meteorological Institute.

The global horizontal and in-plane incident solar radiation were measured using CMP11 pyranometers, the same as are used by weather stations across France, and a common choice for the monitoring of BIPV systems. Local wind conditions were recorded by a roof-mounted ultrasonic sensor.

Each measure was recorded with a UTC timestamp that was resynchronised on a daily basis with a time server. The data stream of each BIPV array was relayed by MODBUS data protocol, managed by a eWON industrial rooter fitted in the electrical cabinet of each BIPV test stand. These devices were configured to send daily data files by FTP to a common server, from which a HTTP connection to each eWON device was available for monitoring and reconfiguration. In practice, the ability to locally store data contributed significantly to the quality of data recovery, whilst offering additional capabilities such as the sending of alarm notifications by email. Raw data were imported into a MySQL database for post-treatment, re-calibration and analysis.

For the validation of thermal and electrical models, filtered data samples were extracted from the database using MySQL requests before being formatted for use with TRNSYS17 software. In the following sections, a selection of four consecutive days in May 2011 is used to demonstrate the performance of each model.

RESULTS

Thermal model performance

Figures 4 and 5 present the simulated and measured PV modules mean temperatures for two BIPV benches. A good qualitative agreement is observed for the short timescale variations in array temperature. The relative errors vary from 0.7% to 2.4% for the test bench called BIPV5 and between 0 and 2% on the BIPV9 test bench. Thus, for both test benches, the thermal model seems to describe quite satisfactorily the thermal behaviour of BIPV systems. Model-data discrepancies are specifically due to difficulties in assessing the air mass flow rate in natural ventilation at the underside of the PV modules along the air gap.

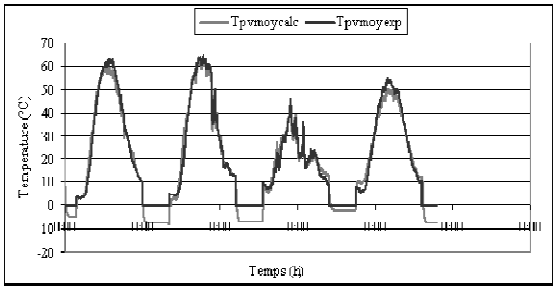

Figure 4 Calculated and measured PV modules mean temperatures comparison for BIPV5 test bench

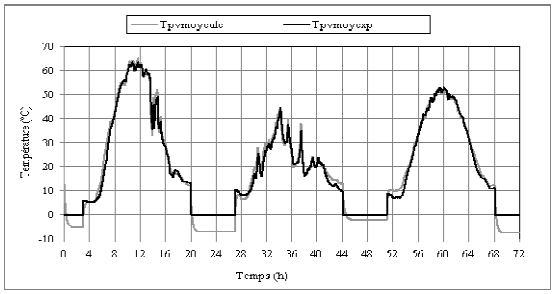

Figure 5 Calculated and measured PV modules mean temperatures comparison for BIPV9 test bench

Electrical model validation

The performance of the selected electrical model is illustrated by Figures 6 and 7. For BIPV5, the mean relative difference on the DC electrical power is 4% for the month of May 2011. For the test bench BIPV9, the model is accurate to 1%. In general, the electrical model overestimates electricity generation. The discrepancy is due in part to systematic uncertainties in the estimation of reference parameters, and in part to the lack of accuracy in the description of temperature and radiation dependence.

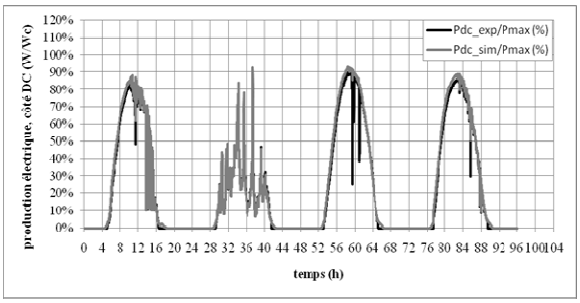

Figure 6 Calculated and measured DC electrical power produced by PV modules on BIPV5 test bench

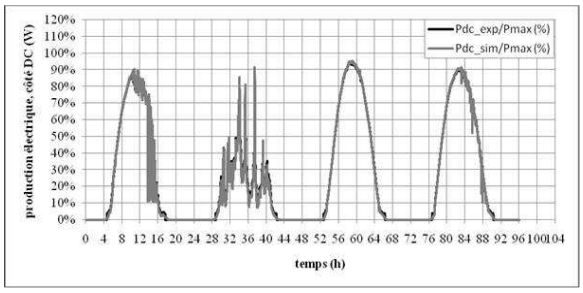

Figure 7 Calculated and measured DC electrical power produced by PV modules on BIPV9 test bench

Since the electrical model has no time dependence, it is also appropriate to display predictions as a function of its input variables. Such a visualisation serves to illustrate the effect of climatic conditions on array performance.

Figure 8 shows the distribution of measured and simulated DC electrical power calculated for one BIPV test bench during the month of May. Eectrical power is displayed as a function of temperature, for four bands in radiation. These graphs illustrate the extent of the data space, and the relationship between operating temperature and incident radiation. The maximum electrical production is obtained for temperatures between 35°C and 70°C and for irradiation between 800 and 1200W / m². For irradiations below 600W / m², electricity production is less than about 0.6 W / Wc. The decline of performance with increasing temperature is visible by inspection of the interface between adjacent bands of data for different radiation levels. Indeed, comparing these interfaces for experimental and simulated data, the temperature dependence of model is clearly overestimated. Model-data errors therefore vary with array temperature.

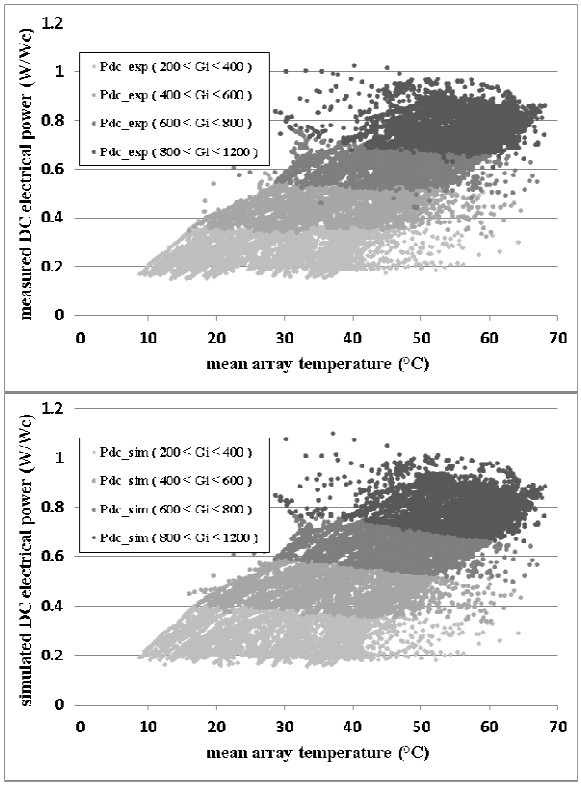

Figure 8 Distribution of measured and calculated electricity as a function of mean PV array temperature and incident solar radiation

Coupled thermal-electrical model

The coupled model was found to be stable for the range of environmental conditions present in the data. Moreover, convergence of the model was achieved on average after nearly 5 iterations, indicating that the coupling between the thermal and the electrical models has a negligible influence on their convergence.

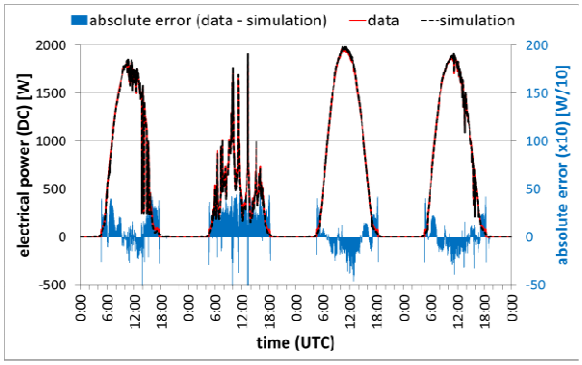

Figure 9 Predicted and measured electrical power for BIPV9, using the coupled thermal-electrical model. Magnified absolute errors are superposed.

The accuracy of the coupled model is demonstrated in Figure 9 for the same period of four days used in

the previous phase of validation. Magnified absolute errors are also illustrated. The accuracy of the model is better for sunny than for cloudy days. The mean error for cloudless days was nearly 2%, whereas for partially cloudy days this precision was reduced to 10%. The 0D and 1D modes of the electrical model returned identical results within the resolution of the data.

Impact of overall thermal conductance on electrical performance

The thermal performance of a BIPV system can be characterised by an equivalent global thermal conductance, Kth, defined as the inverse of the mean variation in array temperature relative to the ambient air temperature resulting from the dissipation of absorbed solar flux. This can be demonstrated by reducing the energy balance of an individual BIPV system to a one-dimensional problem, comprising a single heat source and two heat sinks (convective coupling to ambient air and radiative coupling to the sky):

$$H_{rad}(T_a - T_m) + H_{conv}(T_s - T_m) + (\alpha - \eta)G_i = m\frac{dT_m}{dt} \qquad (11)$$

By regrouping terms involving Tm and introducing Kth=Hrad+Hconv, the global conductance of the BIPV system, a simplified transient model is obtained.

$$K_{th}(T_a - T_m) + H_{rad}(T_s - T_a) + (\alpha - \eta)G_i = m\frac{dT_m}{dt} \qquad (12)$$

In this form, H_{rad} includes form factors and the emissivity of PV modules. Note also that the convective transfer coefficient also includes exchanges to the rear, which are themselves modulated by the radiative exchange between the rear side of the modules and the roof surface (or insulation), and clearly also the local wind conditions. The formulation also assumes that the transient terms result from local thermal inertias, and hence the heat capacity of the modules. Indeed, the thermal inertia of all structures and insulation contribute implicitly to m. In contrast, H_{rad} uniquely describes radiative heat transfer between the external module surface and the sky.

Equation 12 can be solved using experimental data either for the stationary case (m=0) via the linear regression of aggregated hourly data, or for the transient case (m=0), with the help of inverse method for example using the Levenberg-Marquardt method applied to minute-wise data spanning a single day.

Figure 10 presents experimental estimates of the mean Kth for the seven BIPV test stands available to the project Performance BIPV. For each bench, the mean of daily Kth measurements covering an 11-month period, calculated using static and transient models. A clear systematic discrepancy is visible between the two definitions of Kth.

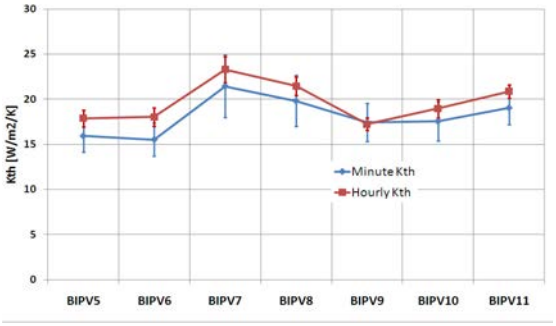

Figure 10 Comparison of K_{th} according to two models: a stationary thermal model using hourly data (red points), and a transient thermal model using minute-wise data (blue points). For each technology K_{th} has been averaged of a period of 11 months, with error bars indicate variability.

Test benches 5, 6, 9 and 10 represent fully-integrated systems (the BIPV systems replace part of the roof structure), and test benches 7, 8 and 11 comprise classical integration configurations where the BIPV system is attached to a complete roof. In terms of K_{th}, the difference between these two forms of integration amounts to around 5 W/m²/K: Kth ranges from 18 W/m²/K for fully integrated systems, to 25 W/m²/K for simple integration configurations. Test benches 8 and 11 have identical configurations but different sites. The similarity of their results suggests that Kth is a reasonably robust measure of thermal characteristics.

Table 1 Simulated annual electricity production of BIPV5 as a function of K_{th}. Horizontal lines indicate the experimentally observed range in K_{th}

K_{th} [W/m²/K]	Production [kWh]	Loss [%]
10	5220	-17.4
12	5431	-12.0
14	5579	-9.9
16	5690	-7.7
18	5775	-6.1
20	5843	-4.9
22	5898	-3.9
24	5944	-3.1
26	5983	-2.5
28	6016	-1.9
30	6045	-1.9
inf.	6130	ref

The thermal-electrical model developed during the present study was employed to estimate the impact of such differences in Kth in terms of electrical performance. Table 1 shows the result of varying Kth while keeping all other parameters constant. The observed difference in conductance corresponds to nearly 5% variation in annual electricity production which is lower or at the same level of uncertainty as

irradiation uncertainty if standard meteorological data base are used.

CONCLUSION

A coupled thermal and electrical model for BIPV systems has been presented. Each part of the model was independently validated using monitoring data on BIPV test benches representative of rooftop systems available in France in 2010. In terms of array temperatures, the thermal model was found accurate to within 2%, and able to reproduce variations on a timescale of one minute. The performance of the electrical model at worst was accurate to 4% in terms of electrical power.

The coupled model permits to provide a fast and robust calculation of power generation using thermo aeraulic internal properties determined with CFD, incident radiation, ambient temperature and wind speed as inputs. The accuracy of the model varied from 2% for sunny days to 10% for cloudy days. Errors were mainly due to an incomplete description of PV modules temperature and absorbed radiation dependence. This is further illustrated by the parametric visualisation of the electrical model for the month of May, which shows that the systems consistently operate away from standard test conditions. Accuracy can be enhanced by improving the electrical description of performance, for example by including system level losses.

NOMENCLATURE

Kj,l = conductance between nodes j and l (W/K)
Ti = temperature at node i (°C)
q = density of the thermal flux absorbed by PV modules (W/m²)
Ta = air ambient temperature (°C)
Ts = sky temperature (°C)
$Tgnd$ = ground temperature (°C)
m = air mass flow rate at the exit of the gap (kg/s)
Cp = air specific heat (J/(kg.K))
β = coefficient of thermal expansion of air (K^{-1})
ρ = air density (kg/m³)
V = wind velocity (m/s)
Li = length of the finite volume I (m)
ΔCp = wind pressure coefficient difference between the inlet and the outlet of the air gap,
g = gravity constant (m/s)
Rei = Reynolds number at finite volume I (-)
H = width of the air gap (m)
X = singular pressure loss coefficient resulting from the cavity inlets (-)
f = coefficient of friction for zone i (-)
Tmo,i, T_c, Tm = PV module temperature (°C)
α = absorptance of PV modules (-)
γ = ideality factor of the junction (-)
η = temperature-dependent solar cell operating efficiency (-)
I_L = photocurrent (A)
I_0 = saturation current of the diode (A)
G_i = incident solar radiation (W/m²)
k = Boltzmann constant ($1.381\ 10^{-23}$ J/K)
R_s = series resistance (Ω)
R_{sh} = shunt resistance (Ω)
H_{conv} = thermal conductance by convection
H_{rad} = thermal conductance by radiation
Kth = equivalent thermal conductance

ACKNOWLEDGEMENT

This project supported by the Research National Agency is a collaboration between CSTB, CEA, CNRS, Transénergie and Cythelia. The authors thank the private companies implied on the project.

REFERENCES

Barker, G., Norton, P. 2003. Building America System Performance Test Practices: Part 1 - Photovoltaic Systems.

Bazilian, M.D., Leenders, F., Van Der Ree, B.G.C., Prasad, D. 2001. Photovoltaic cogeneration in the built environment, Solar Energy.

Brinkworth, B.J., Marshall, R.H., Ibarahim, Z. 2000. A validated model of naturally ventilated PV cladding. Solar Energy.

Chow, T.T. 2003. Performance analysis of photovoltaic-thermal collector by explicit dynamic model, Solar Energy.

Department for Communities and Local Government 2010. Code for Sustainable Homes Technical Guide 2010, United Kingdom, online: "http://www.planningportal.gov.uk/uploads/code_for_sustainable_homes_techguide.pdf, accessed 09/2012"

De Soto, W., Klein, S.A., Beckman, W.A. 2006. Improvement and Validation of a Model for Photovoltaic Array Performance, Solar Energy.

Duffy, J.A, Beckman, W.A. 1991. Solar Engineering of Thermal Processes, second Ed. John Wiley & Sons, New York.

European Commission. 2010. Energy 2020 - A strategy for competitive, sustainable and secure energy, Brussels, Belgium, online: "http://ec.europa.eu/energy/energy2020/energy2020_en.htm, accessed 2012"

Fuentes, M.K. 1987. A simple thermal model for flat-plate photovoltaic arrays, SANDIA report SAND85-0330.

Ingersoll, J. G. 1986. Simplified Calculation of Solar Cell Temperatures in Terrestrial Photovoltaic Arrays, Journal of Solar Energy Engineering.

Leloux, J., Narvarte, L., Trebosc, D. 2012. Review of the performance of residential PV systems in France, Renewable and Sustainable Energy Reviews.

Ministère de l'Ecologie, du Développement Durable et de l'Energie 2012. Règlementation Thermique 2012, France, online: « http://www.developpement-durable.gouv.fr/Chapitre-I-La-reglementation.html, accessed 09/2012 »

Picault, D., Raison, B., Bacha, S., De la Casa, J., Aguilera, J. 2010. Solar Energy.

Sandberg, M., Moshfegh, B. 1998. Ventilated solar roof airflow and heat transfer investigation. Renewable Energy.

Schleicher-Tappeser, R. 2012. How renewables will change electricity markets in the next five years, Energy Policy.

Tiwari, A., Sodha, M.S. Chandra, A. 2006. Solar Energy Materials and Solar Cells.